

# Detection of QRS Complexes in 12-lead ECG using Adaptive Quantized Threshold

V.S. Chouhan<sup>†</sup> and S.S. Mehta<sup>††</sup>

<sup>†</sup>Department of Electronics & Communication Engineering

<sup>††</sup>Department of Electrical Engineering

J.N. Vyas University, Jodhpur, India-342 001

## Summary

The QRS complex is the most prominent wave component within the electrocardiogram. It reflects the electrical activity of heart during the ventricular contraction and the time of its occurrence. Its morphology provides information about the current state of the heart. The identification of QRS-complexes forms the basis for almost all automated ECG analysis algorithms. The presented algorithm employs a modified definition of slope, of ECG signal, as the feature for detection of QRS. A sequence of transformations of the filtered and baseline drift corrected ECG signal is used for extraction of a new modified slope-feature. Two feature-components are combined to derive the final QRS-feature signal. Multiple quantized amplitude thresholds are employed for distinguishing QRS-complexes from non-QRS regions of the ECG waveform. An adequate amplitude threshold is automatically selected by the presented algorithm and is utilized for delineating the QRS-complexes. A QRS detection rate of 98.56% with false positive and false negative percentage of 0.82% and 1.44% has been reported.

## Key words:

ECG, QRS detection, quantized threshold, feature signal.

## 1. Introduction

A standard scalar electrocardiogram is shown in fig.1. It consists of P-wave, PR-interval, PR-segment, QRS-complex, ST-segment, ST-interval and T-wave. The P-wave represents atrial depolarization, the QRS-complex represents left ventricular depolarization and the T-wave represents the left ventricular repolarization.

Various methods, for QRS detection, are found in literature using slope or derivative of ECG signal [1,2], filters [3-9], transforms [10-14], pattern recognition [15,16], Artificial Neural Networks [17,18], Genetic Algorithm [19], Hidden Markov Model [20], morphology operators [21,22], and Support Vector Machines [23-26]. The algorithm reported in this paper uses new modified slope feature and it overcomes the limitations and drawbacks of slope based QRS detection algorithms reported in the literature [1,2].

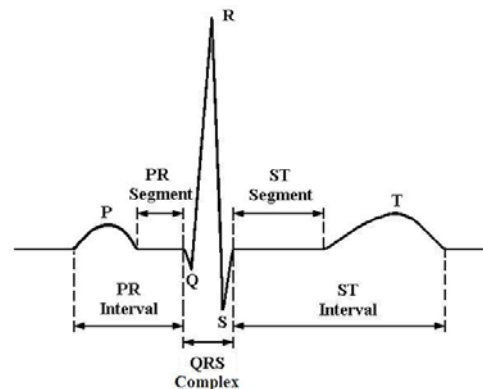


Fig.1 Standard scalar electrocardiogram

In the presented algorithm, filtering procedure based on moving averages [27] provides smooth spike-free ECG signal, which is suitable for slope feature extraction. Reduction of baseline drift is desirable for implementing amplitude-threshold strategy. In this approach, first of all the constituent components of the required feature signal are derived by using a number of transformations on filtered and baseline corrected ECG signal and then extracting the proposed slope feature from these transformed signals. Two constituent components are then combined and refined to yield the desired feature signal  $F_Q$ . The basis of identifying QRS complexes is the amplitude threshold of the QRS-feature signal  $F_Q$ .

## 2. Procedure

The following steps are taken in the presented algorithm for the detection of QRS-complexes:

1. Extract slope feature from the filtered and drift corrected ECG signal, by processing and transforming it, in such a way that the extracted feature signal is prominently enhanced in QRS region and suppressed in non-QRS region.
2. Detect the QRS-complexes by using an adequate value of amplitude threshold of the feature signal  $F_Q$  as detailed in the following steps.

3. Normalize the feature signal, by dividing it by its maximum peak amplitude so that the maximum of the peak value in the entire sample range is referred to as 1, whatever may be the absolute signal peak amplitude.
4. Discard the normalized feature signal below 5% amplitude to ensure the exclusion of small noise that may have been left during filtering. This elimination ensures a low value of False Positive (FP) detections. Wherever the amplitude of the remaining normalized feature signal is above 5% it is marked as QRS candidate using rectangular marking pulses  $C_Q$ .
5. Presented algorithm performs the task of the elimination of weak QRS-candidates on the basis of multiple quantized amplitude-thresholds for the feature signal peak amplitude. If the peak amplitude of the candidate exceeds the threshold it is delineated as QRS-complexes, otherwise, the algorithm eliminates it by reducing the candidate marking pulse amplitude to zero.
6. In the presented algorithm, QRS-complexes are simultaneously detected for 14 quantized amplitude-thresholds, named as  $t_{21}$ ,  $t_{24}$ ,  $t_{27}$ ,  $t_{30}$ ,  $t_{33}$ ,  $t_{36}$ ,  $t_{39}$ ,  $t_{42}$ ,  $t_{45}$ ,  $t_{48}$ ,  $t_{51}$ ,  $t_{54}$ ,  $t_{57}$  and  $t_{60}$  corresponding to 21%, 24%, 27%, 30%, 33%, 36%, 39%, 42%, 45%, 48%, 51%, 54%, 57% and 60% proportion, of the maximum value of the normalized amplitude of the QRS-feature signal  $F_Q$  respectively. The QRS detection results corresponding to each of these thresholds are automatically tabulated, in the lead-wise order, by the algorithm. A range of 14 quantized amplitude-thresholds is chosen so that a large number of observations (QRS-detection results) are available for statistical computations and thus a higher success rate is ensured. The detection with a limited detection rate may be achieved by using lesser number of thresholds.

After obtaining QRS-detection results, for all the 12 single-leads of a case, the statistical computations are performed by the algorithm on the tabulated array of QRS-detection results. This is a 12 rows and 14 columns array automatically tabulated, in the lead-wise order, by the algorithm (Table 1). The 12 rows represent lead-wise QRS-detection results, and the 14 columns represent 14 thresholds.

The median and standard deviation of the QRS-detection results, of all the 12 single-leads for a case, are computed for each of the amplitude threshold of the algorithm. When the standard deviation of detections for a threshold is zero, the detection is correct and the value of the median of detections for that threshold represents the correct number of QRS-complexes in that case. Hence the correct number of QRS-complexes in a case is automatically decided by the algorithm and a reliable QRS-detection is achieved.

Out of multiple quantized amplitude thresholds at least one threshold, in most of the cases, correctly detects all the QRS-complexes without failing. The results of QRS-detection, with this particular threshold, are automatically selected by the algorithm as *final QRS-detection*, on the basis of zero value of the standard deviation of the detection results. This makes the presented algorithm virtually adaptive, that is, an adaptive amplitude threshold is automatically selected out of many quantized thresholds.

In the cases, where QRS-detections are correct (or standard deviation is zero) for more than one quantized threshold, the results of the first threshold (in ascending order) are taken as the final detection. Hence, the presented algorithm may be named as adaptive quantized amplitude threshold strategy or simply adaptive threshold strategy, where the adaptive value of the amplitude threshold is in steps (quantified) rather than being continuous. However, if a zero value of the standard deviation of the QRS-detection results is not obtained for any threshold for the case under investigation, the detections with minimum value of the standard deviation among 14 quantized thresholds is automatically selected as the final QRS-detection result by the algorithm.

The present work has been tested on CSE ECG database [28], which contains 125 cases of 12-lead simultaneously recorded ECG of 10 seconds duration each, sampled at a rate of 500 samples/sec. Thus each of the 1500 (125x12) records has 5000 sampling instants.

### 3. Algorithm For Feature-Extraction

1. Acquire filtered and drift reduced ECG signal  $S(n)$ , (Fig. 2a).  
Where,  $n = 1, 2, 3, \dots, 5000$ , for 5000 samples of ECG signal for each lead of a case under investigation.
2. Derive transformed signal  $TS1(n)$  by squaring the signal  $S(n)$  at each sampling instant  $n$  (Fig. 2b):  
$$TS1(n) = S(n) * S(n); \quad n=1, 2, \dots, 5000 \quad \dots (1)$$
3. Evaluate gradient 'G1' of 'TS1' by using a rectangular sliding window, by the following relation (Fig. 2c):  
$$G1(n) = TS1_{\max}(w) - TS1_{\min}(w);$$
  
$$n=1, 2, \dots, 5000 \quad \dots (2)$$
  
Where,  $w$  is a sliding window of 11 sample points' size from  $(n-5)$  to  $(n+5)$ , with center at  $(n)$  the  $n^{\text{th}}$  sample point.  $TS1_{\max}$  is the maximum value of TS1 signal within this window and  $TS1_{\min}$  is the minimum value of TS1 signal within this window – *thereby providing the steepest windowed gradient*.
4. Compute filtered value  $FG1$  of the gradient  $G1$  to smoothen it (Fig. 2d) by moving averages method

with a rectangular sliding window of 11 sample points' size from (n-5) to (n+5), with center at (n):

$$FG1(n) = \frac{1}{11} \sum_{i=n-5}^{n+5} G2(i)$$

$$n=1, 2, \dots, 5000 \quad \dots (3)$$

5. Compute the normalized values of S, TS1, G1 and FG1 by dividing their all the sample values by their respective maximum peak amplitude so that the unipolar values fall between 0 and 1 and the bipolar values between -1 and 1. Plot these normalized values as seen in Fig. 2.

6. Derive transformed signal 'TS2' by evaluating the following sigmoid function at the signal sample points (Fig. 3b):

$$TS2(n) = 1 - \{2/(e^{2S(n)}+1)\};$$

$$n=1, 2, \dots, 5000 \quad \dots (4)$$

7. Evaluate gradient 'G2' of 'TS2' with the method of step 3 above (Fig. 3c):

$$G2(n) = TS2_{max}(w) - TS2_{min}(w);$$

$$n=1, 2, \dots, 5000 \quad \dots (5)$$

8. Filter the gradient values by moving averages method to evaluate filtered gradient 'FG2' with the method of step 4 above (Fig. 3d).

9. Compute the normalized values of TS2, G2 and FG2 by dividing all their samples by their respective maximum peak amplitude (Fig. 3).

10. Derive transformed signal 'TS3' by multiplying the ECG signal 'S' with filtered gradient 'FG2' (Fig. 4b):

$$TS3(n) = FG2(n) * S(n); \quad n=1, 2, \dots, 5000 \quad \dots (6)$$

The advantage of this multiplication can be clearly seen in fig. 4(b) that the tall and prominent T-waves have almost disappeared with respect to QRS complexes.

11. Evaluate gradient 'G3' of 'TS3' with the method of step 3 above (Fig. 4c):

$$G3(n) = TS3_{max}(w) - TS3_{min}(w);$$

$$n=1, 2, \dots, 5000 \quad \dots (7)$$

12. Filter the gradient values by moving averages method to evaluate filtered gradient 'FG3' with the method of step 4 above (Fig. 4d).

13. Compute the normalized values of TS3, G3 and FG3 by dividing all their samples by their respective maximum (Fig. 4).

14. Attain the desired feature signal  $F_Q$  by using the two constituent feature signals, namely, the filtered gradients 'FG1' and 'FG3' (Fig. 5d):

(a) Derive transformed signal TS4 by adding filtered gradients FG1 and FG3:

$$TS4(n) = FG1(n) + FG3(n); \quad n=1, 2, \dots, 5000 \quad \dots (8)$$

(b) Derive TS4m by applying median correction on TS4, that is, shifting TS4 vertically by subtracting median value of TS4 from it:

$$TS4m(n) = TS4(n) - m; \quad n=1, 2, \dots, 5000 \quad \dots (9)$$

Where,  $m = \text{median}(TS4(n))$ .

(c) Derive the Pre-final feature signal  $Pre\_F_Q$  by normalizing TS4m (Fig. 5c):

$$Pre\_F_Q(n) = TS4m(n)/\max(\text{abs}(TS4m(n)));$$

$$n=1, 2, \dots, 5000 \quad \dots (10)$$

Where,  $\max(\text{abs}(TS4m(n)))$  is the maximum peak amplitude of absolute value of TS4m in the entire sampling interval from 1 to 5000. This fixes the extreme values of amplitude of  $Pre\_F_Q$  between -1 and +1.

(d) Derive the desired final QRS feature signal  $F_Q$  by retaining the amplitude values of  $Pre\_F_Q$  exceeding 5% of its maximum peak amplitude and reducing the remaining to zero (Fig. 5f):

$$F_Q(n) = \begin{cases} Pre\_F_Q(n), & \text{if } Pre\_F_Q(n) > 0.05 \\ 0, & \text{otherwise} \end{cases}$$

$$n=1, 2, \dots, 5000 \quad \dots (11)$$

The signal  $F_Q$  is the proposed feature signal (fig. 5f) employed for identifying the QRS candidates and detecting the true QRS-complexes out of these candidates within the ECG signal.

The effect of applying sigmoid function on signal  $S(n)$  can be seen explicitly in Fig. 3 (b) in the form of the Transformed Signal  $TS2(n)$ :

- (i) It enhances slope of the steepest parts of the signal and reduces slope of the remaining parts of the signal  $S(n)$ , where  $n$  is the  $n^{\text{th}}$  sampling instant.
- (ii) According to property of sigmoid function: as  $S(n)$  approaches to  $-\infty$ ,  $TS2(n)$  goes to -1, and as  $S(n)$  approaches to  $+\infty$ ,  $TS2(n)$  goes to +1.

As a result, the smaller but sharp and peaky P-waves and QRS are enhanced in magnitude as compared to the tall T-waves with greater magnitude but not sharp in nature, as seen in fig. 3(b).

#### 4. Algorithm for QRS-Detection

1. Demarcate ' $F_Q$ ' by QRS candidate marking pulses  $C_Q$  of unit amplitude, marking the QRS candidate region, using the relation:

$$C_Q(n) = \begin{cases} 1, & \text{if } F_Q(n) > 0.05 \\ 0, & \text{otherwise} \end{cases}$$

$$n = 1, 2, \dots, 5000 \quad \dots (12)$$

Demarcated ' $F_Q$ ' represent candidate QRS complexes.

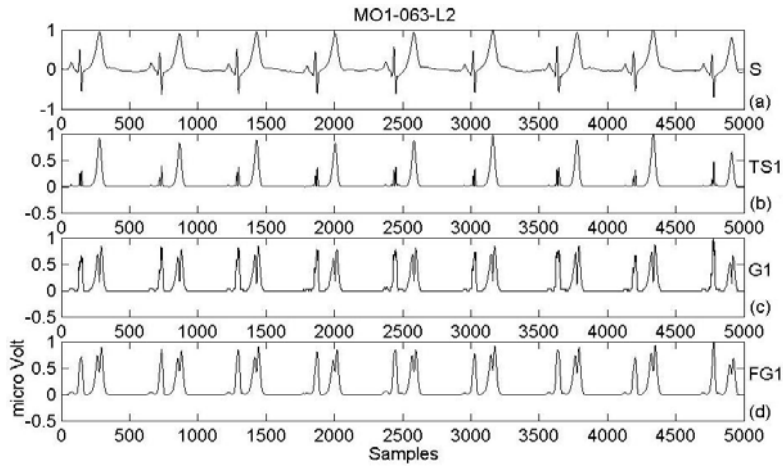


Fig. 2 Normalized values of (a) Filtered and baseline drift corrected ECG signal S (b) Squared signal TS1 (c) Gradient G1 of TS1 (d) FG1: Gradient G1 after filtering – the first constituent component of QRS-feature signal  $F_Q$

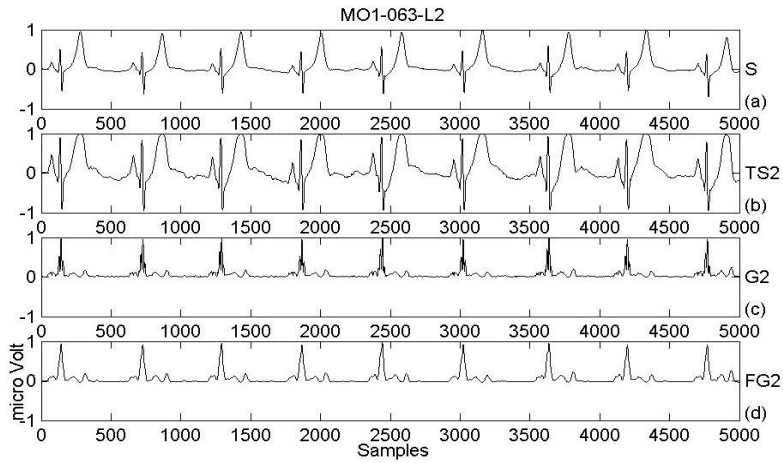


Fig. 3 Normalized values of (a) Filtered and baseline drift corrected ECG signal S (b) Transformed signal TS2 by applying sigmoid function on signal S (c) G2: Gradient of TS2 (d) FG2: Gradient G2 after filtering – intermediate component of the QRS feature signal  $F_Q$

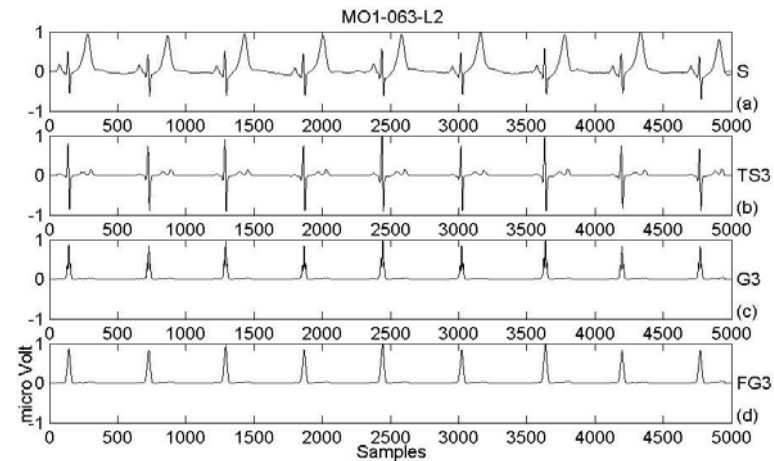


Fig. 4 Normalized values of (a) Filtered and baseline drift corrected ECG signal S (b) Transformed signal TS3: obtained by multiplying TS2 with signal S (c) G3: Gradient of TS3 (d) FG3: Gradient G3 after filtering – the second constituent component of the QRS-feature signal  $F_Q$

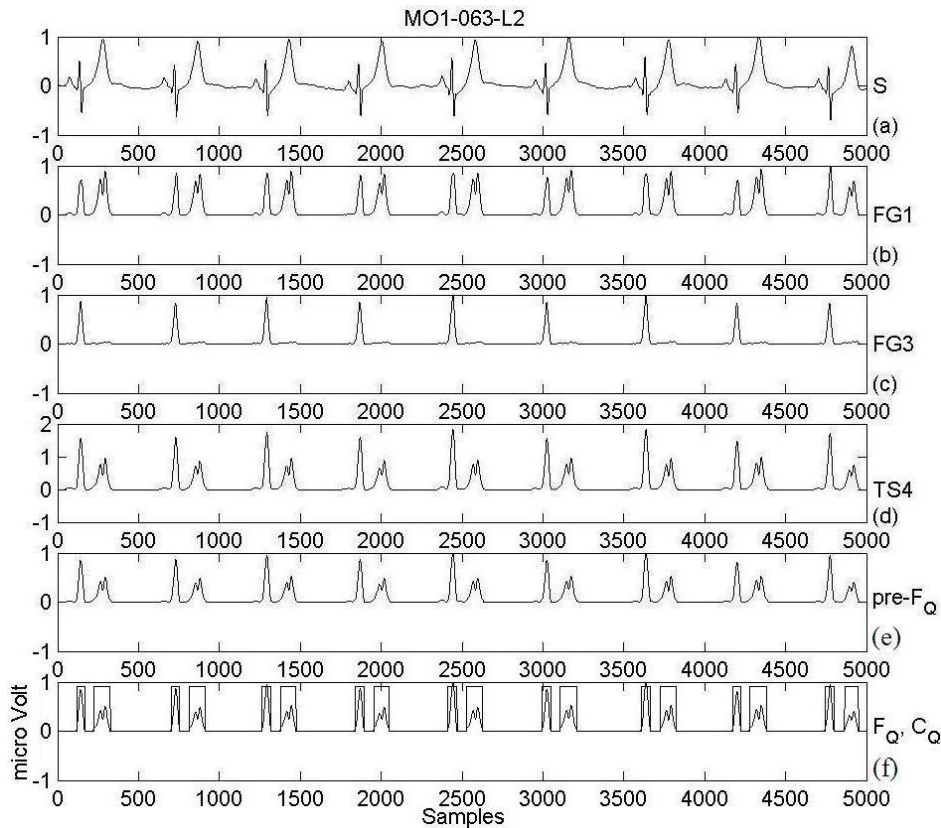


Fig. 5 Normalized values of (a) Filtered and baseline drift corrected ECG signal S (b) FG1 – First constituent component of the feature (c) FG3 – Second constituent component of the feature (d) Transformed signal TS4: obtained by adding FG1 and FG3 in order to attain  $F_Q$  (e) Pre- $F_Q$ : The pre-final QRS feature signal (f) The pre-final QRS feature signal  $F_Q$

2. Define a range of normalized adaptive amplitude-thresholds  $t_{21}, t_{24}, t_{27}, t_{30}, t_{33}, t_{36}, t_{39}, t_{42}, t_{45}, t_{48}, t_{51}, t_{54}, t_{57}$  and  $t_{60}$  representing 0.21, 0.24, 0.27, 0.30, 0.33, 0.36, 0.39, 0.42, 0.45, 0.48, 0.51, 0.54, 0.57 and 0.60 fractional proportion of the maximum peak value of normalized  $F_Q$ . Testify for QRS-membership, among all QRS-candidates, within each demarcated ' $F_Q$ '.
3. Taking one threshold at a time, testify the crossing of the threshold by the peak value of ' $F_Q$ ' within all the QRS-candidate marking pulses  $C_Q$  in the entire sampling duration from 1<sup>st</sup> to 5000<sup>th</sup> sampling instants as follows:

$$\begin{aligned}
 &\text{if } F_{Q,\max}(\text{cmp}) < t \\
 &\quad D_Q(\text{cmp}) = 0 \quad \text{else } D_Q(\text{cmp}) = 1; \\
 &\text{end} \\
 &\dots (13)
 \end{aligned}$$

Here,  $t$  = thresholds from  $t_{21}$  to  $t_{60}$  as described above

$\text{cmp}$  = QRS-candidate marking pulses duration from  $C_{Q\_begin}$  to  $C_{Q\_end}$ , in the sampling range of 1 to 5000

$F_{Q,\max}(\text{cmp})$  = maximum value of normalized  $F_Q$  within each marking pulse  $C_Q$

$D_Q(\text{cmp})$  = Detected QRS marking pulse, which is nothing but a QRS candidate marking pulse that is preserved by assigning '1' if designated threshold is crossed; and eliminated by assigning '0' if the designated threshold is not crossed by the peak amplitude of ' $F_Q$ ' within (cmp).

The number of adaptive thresholds mentioned above may be reduced with some reduction in rate of successful QRS-detections but inclusion of all the above thresholds help in more reliable automated QRS-detection, based on statistical calculations (refer step 5 & 6 of this algorithm).

4. Demarcate  $D_Q$  for all the 12 leads of a given case, count and list the number of  $D_Q$ , that is, number of QRS detections and compute statistical properties for these number of detections for the case:
  - (a) Median ( $m_1$ ) and Standard Deviation ( $sd_1$ ) of number of QRS detections for all the 12 leads of the case
  - (b) Median ( $m_2$ ) and Standard Deviation ( $sd_2$ ) of medians of QRS detections

- (c) Median (m3) & Standard Deviation (sd3) of standard deviations of QRS detections (that is, median & standard deviation of sd1 for t21, t24, ..., t60)
- 5. Select all the QRS detections, demarcated by QRS-detection marking pulses  $D_Q$  of the given case with:
  - (a) Minimum value of standard deviation sd1
  - (b) The corresponding value of median m1 equal to the correct and reliable number of QRS complexes  $Q_N$  in that case, evaluated by algorithm (Section 6)
  - (c) Demarcate the first (in the order of columns of Table 1) column out of these QRS detections with QRS Marking Pulses  $MP_Q$ . That is, the first out of many correct QRS detections demarcated by  $D_Q$  are declared as the *final QRS detection* and the

corresponding marking pulses are designated as  $MP_Q$ .

**Note:** The cases in which the value of both m3 and sd3 are zero, in those cases all the QRS detections, for thresholds t21, t24, ..., t60, are correct and the following unique condition holds good for such cases:

$$m1 = m2 = \text{unambiguous number of QRS complexes in that case.} \dots (14)$$

- 6. Use these final QRS marking pulses  $MP_Q$  to delineate the given ECG signal. The portions of the ECG signal within these marking pulses  $MP_Q$  are the detected QRS complexes with the presented algorithm.

Table 1 Number of QRS detections, for all the 12 leads of the case MO1\_063, and their statistical parameters under each threshold.

Column →		1	2	3	4	5	6	7	8	9	10	11	12	13	14
Row ↓		Thresholds													
Lead ↓		t21	t24	t27	t30	t33	t36	t39	t42	t45	t48	t51	t54	t57	t60
1	L1	9	9	9	9	9	9	9	9	9	9	9	9	9	9
2	L2	18	18	18	18	18	18	17	16	16	15	10	9	9	9
3	L3	9	9	9	9	9	9	9	9	9	9	9	9	9	9
4	aVL	9	9	9	9	9	9	9	9	9	9	9	9	9	9
5	aVR	9	9	9	9	9	9	9	9	9	9	9	9	9	9
6	aVL	9	9	9	9	9	9	9	9	9	9	9	9	9	9
7	V1	9	9	9	9	9	9	9	9	9	9	9	9	9	9
8	V2	9	9	9	9	9	9	9	9	9	9	9	9	9	9
9	V3	9	9	9	9	9	9	9	9	9	9	9	9	9	9
10	V4	9	9	9	9	9	9	9	9	9	9	9	9	9	9
11	V5	9	9	9	9	9	9	9	9	9	9	9	9	9	9
12	V6	9	9	9	9	9	9	9	9	9	9	9	9	9	9
13	Median m1	9	9	9	9	9	9	9	9	9	9	9	*9	9	9
14	Std. Dev. sd1	2.6	2.6	2.6	2.6	2.6	2.6	2.3	2.0	2.0	1.7	0.3	*0	0	0

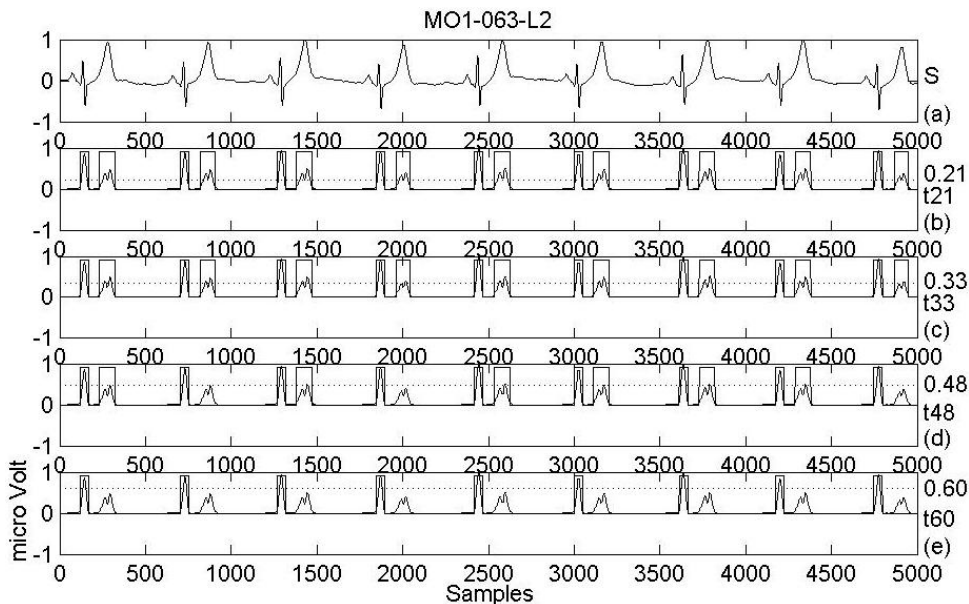


Fig. 6 Normalized values of (a) Filtered and baseline drift corrected ECG signal S (b) QRS detection with 21% threshold t21 (c) QRS detection with 33% threshold t33 (d) QRS detection with 48% threshold t48 (e) QRS detection with 60% threshold t60

### 5. Algorithm for Computation of Correct Number of QRS-Complexes

1. Compute median  $m1$  and standard deviation  $sd1$  under each of the 14 columns of QRS detections already tabulated in Table 1.
2. Compute median  $m2$  and standard deviation  $sd2$  of the row containing all  $m1$  values.
3. Compute median  $m3$  and standard deviation  $sd3$  of the row containing all  $sd1$  values.
4. Compute correct number of QRS complexes  $Q_N$  for a given case by applying the following condition:

$$\begin{aligned} &\text{if } (sd2 < 1) \ \& \ (m3 < 1) \\ &\quad Q_N = m2; \\ &\text{End} \end{aligned} \quad \dots (15)$$

The number of QRS complexes  $Q_N$ , computed automatically by the algorithm were verified manually for all the 125 cases of the CSE database dataset-3 and found to be correct in cent percent cases. *Hence, the automatic computation of the number of QRS complexes, for a given case, by the algorithm presented in this paper, is correct and reliable.*

For this reason, the number of false negative (FN) and false positive (FP) computations and therefore the performance evaluation of the algorithm are credible.

### 6. Automatic Selection of Final QRS-Detection Result

In most of the cases, the QRS-complexes are correctly detected by multiple values of thresholds. One out of these detections is automatically selected as the final QRS-detection result, for delineating the detected QRS-complexes and displaying the delineated result graphically, using the following algorithm:

- Select the row of standard deviations  $sd1$  and compute their minimum value

- Select the median value  $m1$  corresponding to the first of these minimum  $sd1$ , if this  $m1$  is equal to  $Q_N$  – the *correct number of QRS-complexes* in the case
- Select all the detected QRS-complexes corresponding to its column number, that is, the column with the same index number as that of  $m1$  and  $sd1$  in the preceding step above – this decides that the *final QRS-detection* is done by which threshold.
- Designate the corresponding detected QRS marking pulses  $D_Q$  as the *final QRS-detection* marking pulses  $MP_Q$ .

### 7. Case Study

Fig. 7 shows the QRS detection in presence of tall P-waves and smaller T-waves. Both the feature signal components FG1 and FG3 are a bit larger in P-wave region and hence the final feature signal  $F_Q$  contains considerable amplitude in P-wave region. This leads P-waves to be considered as potential QRS candidates by the algorithm. But finally the tall and prominent P-waves have been successfully rejected of their candidature all of the QRS complexes are correctly detected by the algorithm.

### 8. Analytical Results of QRS Detection

Table 2 presents combined overall results of final QRS-detections for the entire CSE library dataset-3 The table presents the performance of detections indicating false negative (FN), false positive (FP) and true positive (TP) detections.

Two standard parameters of measuring the performance of the detection results, namely detection rate ( $DR$ ) and positive predictivity ( $+P$ ), are also presented in Table 2.

This can be clearly seen from the table that the false negative and false positive percentage is extremely low, that is, 1.44% and 0.82% respectively.

Table 2 Combined overall results of final QRS-detection for the entire CSE dataset-3

Actual No. of QRS complexes	True Positive <b>TP</b>	False Negative <b>FN</b>	False Positive <b>FP</b>	Total Errors <b>TE</b>	Percent FN	Percent FP	Detection Rate <b>DR</b>	Positive Predictivity <b>+P</b>
17988	17729	259	148	407	1.44%	0.82%	98.56%	99.18%

$$DR = TP/(TP+FN), \ +P = TP/(TP+FP), \ TE = Total Errors = FN + FP$$

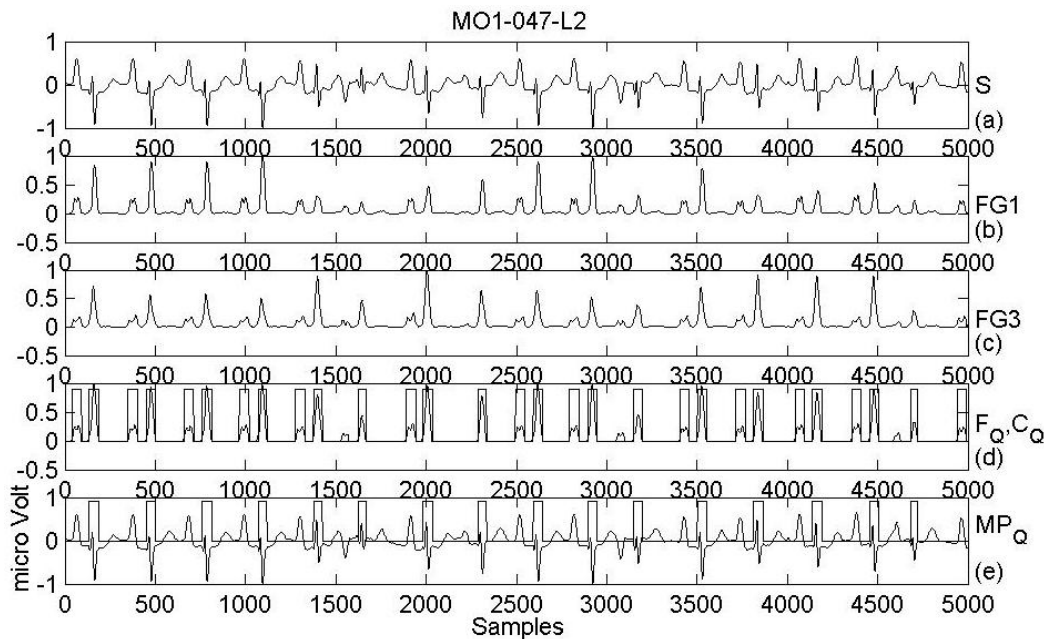


Fig. 7 (a) Filtered and baseline drift corrected ECG signal S (b) FG1 – First constituent component of the feature (c) FG3 – Second constituent component of the feature (d) Final QRS feature signal  $F_Q$ , QRS candidate marking pulse  $C_Q$  (e) Finally detected QRS-complexes delineated by QRS marking pulse  $MP_Q$

## 9. Conclusion

The paper presents a derivative based new approach for QRS detection in ECG signals. The algorithm reported overcomes various shortcomings of the derivative based algorithms reported in the literature. It has been tested on all leads of 125 cases of CSE ECG library dataset 3 containing wide varieties of QRS morphologies of normal as well as 32 categories of cardiac ailments.

It has detection rate and positive predictivity of 98.56% and 99.18% respectively.

The information obtained by this method is very useful for ECG classification and cardiac diagnosis. This information can also serve as an input to a system that allows automatic cardiac diagnosis.

## References

- [1] B.U. Kohler, C. Hennig and R. Orglmeister, "The principles of software QRS detection", IEEE Engineering in Medicine and Biology Magazine, vol. 21, no. 1, pp. 42-57, Jan.-Feb. 2002.
- [2] M.L. Ahlstrom and W.J. Tompkins, "Automated high-speed analysis of holter tapes with microcomputers," IEEE Trans. Biomed. Eng., vol. 30, pp. 651-657, Oct. 1983.
- [3] M.L. Ahlstrom and W.J. Tompkins, "Digital filters for real-time ECG signal processing using microprocessors", IEEE Trans. Biomed. Eng., vol. BME-32, no. 9, pp. 708-713, Sept. 1985.
- [4] G. Tremblay and A.R. LeBlanc, "Near-optimal signal preprocessor for positive cardiac arrhythmia identification", IEEE Trans. on Biomed. Engg., vol.32, no.2, pp.141-151, Feb. 1985.
- [5] Q. Xue, Y.H. Hu and W.J. Tompkins, "Neural-network-based adaptive matched filtering for QRS detection," IEEE Trans. Biomed. Eng., vol. 39, no. 4, pp. 317-329, April 1992.
- [6] Y. Sun, S. Suppappola and T.A. Wrublewski, "Microcontroller-based real-time QRS detection," Biomed. Instrum. Technol., vol. 26, no. 6, pp. 477-484, 1992.
- [7] S. Suppappola and Sun Ying, "Nonlinear transforms of ECG signals for digital QRS detection: a quantitative analysis", IEEE Trans. Biomed. Eng., vol. 41, pp. 397-400, April 1994.
- [8] A. Ligtenberg and M. Kunt, "A robust-digital QRS-detection algorithm for arrhythmia monitoring," Comput. Biomed. Res., vol. 16, pp. 273-286, 1983.
- [9] P.S. Hamilton and W.J. Tompkins, "Adaptive matched filtering for QRS detection," in Proc. Annual Int. Conf. IEEE Eng. in Medicine and Biology Society, New Orleans, LA, U.S.A., pp. 147-148, 1988.
- [10] I.S.N. Murthy and U.C. Niranjana, "Component wave delineation of ECG by filtering in the fourier domain", Medical & Bio. Engg. and Compu., vol.30, pp.169-176, March 1992.
- [11] I.S.N. Murthy and G.S.S.D. Prasad, "Analysis of ECG from pole-zero models", IEEE Trans. on Biomed. Engg., vol.39, no.7, pp.741-751, July 1992.



- [12] M.E. Nygard and L. Sornmo, "Delineation of the QRS complex using the envelope of the ECG," *Med. Biol. Eng. Comput.*, vol. 21, pp. 538-547, March 1983.
- [13] F. Gritzali, "Towards a generalized scheme for QRS detection in ECG waveforms," *Signal Processing*, vol. 15, pp. 183-192, 1988.
- [14] F. Gritzali, G. Frangakis and G. Papakonstantinou, "A comparison of the length and energy transformations for the QRS detection," in *Proc. 9<sup>th</sup> Annual Conf. IEEE Engineering in Medicine and Biology Society*, Boston, MA, pp. 549-550, 1987.
- [15] S.S. Mehta S.C. Saxena and H.K. Verma, "Computer aided interpretation of ECG for diagnostics", *International Journal of System Science*, vol. 27, pp.43-58, 1996.
- [16] P. Trahanias and E. Skordalakis, "Primitive pattern selection and extraction in ECG waveforms", *Proceedings of 8<sup>th</sup> Int. Conference on Pattern Recognition*, IEEE Computer Society, pp. 380-382, 1986.
- [17] Y. Suzuki, "Self-organizing QRS-wave recognition in ECG using neural networks," *IEEE Trans. Neural Networks*, vol. 6, pp. 1469-1477, 1995.
- [18] G. Vijaya, V. Kumar and H.K. Verma, "ANN-based QRS-complex analysis of ECG," *J. Med. Eng. Technol.*, vol. 22, no. 4, pp. 160-167, 1998.
- [19] R. Poli, S. Cagnoni and G. Valli, "Genetic design of optimum linear and nonlinear QRS detectors," *IEEE Trans. Biomed. Eng.*, vol. 42, no. 11, pp. 1137-1141, Nov. 1995.
- [20] D.A. Coast, R.M. Stern, G.G. Cano and S.A. Briller, "An Approach to Cardiac Arrhythmia Analysis Using Hidden Markov Models", *IEEE Transactions on Biomedical Engineering*, vol. 37, no. 9, pp. 826-836, Sept. 1990.
- [21] P.E. Trahanias, "An approach to QRS complex detection using mathematical morphology", *IEEE Transactions on Biomedical Engineering*, vol. 40, no. 2, pp. 201 – 205, Feb. 1993.
- [22] I. Christov, G.H. German, V. Krasteva, I. Jekova, A. Gotchev and K. Egiazarian, "Comparative Study of Morphological and Time-Frequency ECG Descriptors for Heartbeat Classification", *Medical Engineering and Physics*, pp. 876-887, Nov. 2006.
- [23] H.J. Liu, Y.N. Wang and X.F. Lu, "A Method to Choose Kernel Function and its Parameters for Support Vector Machines", *Proceedings of International Conference on Machine Learning and Cybernetics*, 2005, vol. 7, pp. 4277-4280, 18-21 Aug. 2005.
- [24] S.S. Mehta and N.S. Lingayat, "ECG Pattern Classification using Support Vector Machine", *The Sixth International Conference on Advances in Pattern Recognition*, ISI, Kolkata, India, 2-4 Jan. 2007.
- [25] K. Thadani, Ashutosh, V.K. Jayaraman and V. Sunderarajan, "Evolutionary Selection of Kernels in Support Vector Machines", *International conference on Advanced Computing and Communications*, ADCOM 2006, pp. 19-24, 20-23 Dec. 2006.
- [26] S. Osowski, L.T. Hoai and T. Markiewicz, "Support vector machine-based expert system for reliable heartbeat

recognition", *IEEE Transactions on Biomedical Engineering*, vol. 51, no. 4, pp. 582-589, April 2004.

- [27] V.S. Chouhan and S.S. Mehta, "Total Removal of Baseline Drift from ECG Signal", *Proceedings of International conference on Computing: Theory and Applications*, ICTTA-07, pp. 512-515, ISI, Kolkata, India, 5-7 March, 2007.
- [28] J.L. Willems, "Common Standards for quantitative electrocardiography", *CSE multilead atlas dataset-3*, CSE Project, Leuven, Belgium, pp. 1-341, ACCO Publ. 1988



**Vijay S. Chouhan** was born in India in 1960. He received B.E. degree in Electronics & Communication Engineering and M.E. degree in Digital Communication Engineering from J. N. V. University, Jodhpur (India). He submitted his Doctoral thesis on Biomedical Signal Processing in 2007. Presently he is Associate Professor in the Department of Electronics & Communication Engineering, M.B.M. Engineering College, J. N. Vyas University, Jodhpur. His research interest includes fields of Biomedical Signal Processing, Soft Computing and Digital Communications.



**Sarabjeet S. Mehta** was born in Kolkata, India in 1958. He received the B.E. degree in Electrical Engineering and M.E. degree in Control System from J. N. Vyas University, Jodhpur- Rajasthan (India) in 1980 and 1987 respectively. He received Ph.D. degree in Electrical Engineering from Indian Institute of Technology, Roorkee in 1994. Presently he is Associate Professor and Head, Electrical Engineering Department of M.B.M. Engineering College, J. N. Vyas University, Jodhpur (India). His research interest includes pattern recognition, artificial neural networks, biomedical engineering, soft computing and electrical machines. He is a fellow of Institution of Engineers (India) and life member of Indian Society for Technical Education.